Turkish Journal of Chemistry

http://journals.tubitak.gov.tr/chem/

Research Article

Turk J Chem
(2021) 45: 1463-1475
© TÜBİTAK
doi:10.3906/kim-2102-67

Acetylene hydrochlorination over tin nitrogen based catalysts: effect of nitrogen carbon-dots as nitrogen precursor

Yibo WU[1,2], Fuxiang LI[2,*], Qingbin LI[1], Songtian LI[1], Ganqing ZHAO[1], Xuerong SUN[1], Peisong LIU[1], Guoxv HE[1], Yongjun HAN[1], Liping CHENG[1], Shiying LUO[1]

[1]College of Chemistry and Enviromental Engineering, Pingding Shan University, Pingding Shan, China
[2]College of Chemistry and Chemical Engineering, Taiyuan University of technology, Taiyuan, China

Received: 26.02.2020 • **Accepted/Published Online:** 22.06.2021 • **Final Version:** 19.10.2021

Abstract: The catalysts comprising the main active compounds of Sn-N_x were synthesized using trichlorophenylstannane ($(C_6H_5)Cl_3Sn$), nitrogen carbon-dots (NCDs), and activated carbon (AC) as starting materials, and the activity and stability of catalysts was evaluated in the acetylene hydrochlorination. According to the results on the physical and chemical properties of catalysts (TEM, XRD, BET, XPS and TG), it is concluded that NCDs@AC can increase $(C_6H_5)Cl_3Sn$ dispersity, retard the coke deposition of $(C_6H_5)Cl_3Sn$/AC and lessen the loss of $(C_6H_5)Cl_3Sn$, thereby further promoting the stability of $(C_6H_5)Cl_3Sn$/AC. Based on the characterization results of C_2H_2-TPD and HCl adsorption experiments, we proposed that the existence of Sn-N_x can effectively strengthen the reactants adsorption of catalysts. By combing the FT-IR, C_2H_2-TPD and Rideal-Eley mechanism, the catalytic mechanism, in which C_2H_2 is firstly adsorbed on $(C_6H_5)Cl_3Sn$ to form $(C_6H_5)Cl_3Sn$-C_2H_2 and then reacted with HCl to produce vinyl chloride, is proposed.

Key words: Trichlorophenylstannane, nitrogen carbon-dots, vinyl chloride, acetylene hydrochlorination

1. Introduction

Organotin compounds (OTCs), as one of organometallic compounds [1], have been widely applied to many areas, encompassing anticancer therapy [2–4], biocides [5], stabilizer [6], and catalysts [7–11]. Currently, scientists have proved that alkyl-organotin not only can be used as stabilizer in polymerization vinyl chloride fabrication (PVC) but also can catalyze acetylene hydrochlorination to manufacture vinyl chloride [6,11,12]. The production of PVC in many regions mainly depends on the carbon-supported $HgCl_2$ catalytic acetylene hydrochlorination reaction [13]. However, the prevention and governance of mercury pollution is still a serious problem around the world [14,15]. Therefore, the nonmercuric catalytic acetylene hydrochlorination process for PVC production need to be urgently explored.

Great attentions have been paid to study the tin-based catalysts in the hydrochlorination of acetylene, especially inorganic tin in the past few years. Researchers founded that metal compounds additives, including $BiCl_3$ [16], $ZnCl_2$ [17], $CuCl_2$ [18], $CeCl_3$ [19], $CoCl_2$ [20] and LiCl [21] can effectively improve the stability of inorganic tin-based catalysts. Basing from the study by Deng reported that the deactivation of $SnCl_4$/AC catalysts for acetylene hydrochlorination is due to the high volatility of $SnCl_4$ [16]. Gao et al. reported that the $CoCl_2$ and $BiCl_3$ promoters can effectively lessen the coking formation of $SnCl_4$/AC in acetylene hydrochlorination and improve the stability of $SnCl_4$/AC catalysts [17]. Although $SnCl_2$/AC can rival the catalytic activity of Hg-based catalysts, the key scientific and technological issue of $SnCl_2$/AC catalysts is to improve its stability [16]. Later on, Guo et al. founded that the synergistic effect of $SnCl_2$, $ZnCl_2$ and Tb_4O_7 can strengthen the catalytic performance of $SnCl_2$/AC in the hydrochlorination of acetylene [20]. In our previous work, we reported that LiCl-promoted $SnCl_2$ catalysing acetylene hydrochlorination with considerable stability, originating from the synergistic effect between Sn and Li [21]. Moreover, organotin catalysts, as another kind of tin-based catalysts in acetylene hydrochlorination, have been studied [11,12,22]. There is no research regarding the catalytic mechanism of organotin as catalysts for acetylene hydrochlorination.

Owing to the specified electronic properties and unique chemical characteristics, a series of nitrogen-doped carbon materials as catalyst carries is grabbing more attention in acetylene hydrochlorination [23-25]. For example, Dai et al. synthesized g-C_3N_4/AC as a novel nonmetallic catalyst, which can catalyze acetylene to produce vinyl chloride [23].

* Correspondence: l63f64x@163.com

Afterward, scientists reported that the coexistence of pyridinic nitrogen and pyrrolic nitrogen in nitrogen-doped carbons could strengthen the adsorption of the reactants [24]. Furthermore, Li et al. studied that the enhancement of $AuCl_3$/PPy-MWCNT catalytic performance was due to the electron transfer from N atom in PPy to the Au^{3+} and, thus, improve the hydrogen chloride adsorption [25].

In this paper, nitrogen-carbon quantum dots (NCDs) with distincitive physical and chemical properties [26–30] is used as nitrogen sources in the preparation of tin nitrogen based acetylene hydrochlorination catalysts. Specifically, the aims of this work are to study the effect of NCDs on the performance of $(C_6H_5)Cl_3Sn$-based catalysts for acetylene hydrochlorination and the catalytic mechanism of $(C_6H_5)Cl_3Sn$/AC in acetylene hydrochlorination.

2. Materials and methods

2.1. Materials

Coal-based activated carbon (φ=1.5 mm, l=5 mm) was obtained from Shanxi Xinhua Chemical Company. Trichlorophenylstannane (98.0%) was purchased from TCI (Shanghai) Development Co., Ltd. Citric acid (99.5%), urea (99.0%), ammonium hydroxide (25~28%), and ethanol (99.5%) were obtained from Tianjin Kermel Technology Development Co., Ltd.

2.2. Catalyst preparation

2.2.1. Preparation of NCDs

N-doped carbon quantum dots (NCDs) were prepared by citric acid and urea [31,32]. Specifically, citric acid (2.0 g) and urea (2.0 g) were dissolved in distilled water (15 mL). Then, the mixture was transferred to a Teflon coated stainless-steel autoclave and heated at 160 °C for 7 h. Afterward, the obtained NCDs solution was mixed with ethanol and centrifuged at 8000 rpm for 20 min. Finally, the samples were dried overnight at 80 °C to obtain the purified NCDs powders.

2.2.2. Preparation of NCDs@AC

NCDs (1.0 g), AC (9.0 g) and ammonium hydroxide was mixed in deionized water (20 mL), and the mixture was stirred at a room temperature for 30 min. Then, the mixture was transferred to a Teflon coated stainless-steel autoclave and heated at 200 °C for 8 h. The obtained samples was washed by deionized water and dried at 100 °C overnight. The final solid sample was labeled as NCDs@AC. Carbon support was pretreated by the same procedure, and the obtained carbon sample was denoted as AC.

2.2.3. Preparation of $(C_6H_5)Cl_3Sn$-based catalysts

$(C_6H_5)Cl_3Sn$/NCDs@AC was synthesized using NCDs@AC as support and $(C_6H_5)Cl_3Sn$ as active compounds, respectively. Specifically, $(C_6H_5)Cl_3Sn$ (1.5 g) was dissolved in the appropriate amount of ethanol, and then this impregnation solution was slowly added to NCDs@AC (8.5 g). The obtained heterogeneous solid was dried at 80 °C to get 15%$(C_6H_5)Cl_3Sn$/NCDs@AC. The similar procedure was repeated to prepare the $(C_6H_5)Cl_3Sn$/AC catalysts for comparisons.

2.3. Catalyst characterization

Powder X-ray diffraction (XRD) patterns were carried out on Shimadzu XRD-6000 with Cu Ka radiation (0.15418 nm). All samples were taken at range of 10–80°C. Catalysts were degassed at 150 °C for 4 h, before the nitrogen adsorption/desorption isotherms at –196 °C were analyzed using Quantachrome NOVA 2000e. Fourier transform infrared (FT-IR) spectra were recorded by a Biorad Excalibur FTS 3000 equipped with a DTGS detector. Transmission electron microscopy (TEM) was performed on JEM-2100F instruments at an acceleration voltage of 200 kV, used to study the dispersion of Sn species, and it characterized the morphology of Sn-based catalysts . X-ray photoelectron spectroscopy (XPS) was conducted on EscaLab 250Xi instruments using Al Ka X-ray source and analyzed the valence of element on the surface of support. The spectra were analyzed using XPSPEAK software pack and corrected for changing in using C1s binding energy (BE) as the reference at 284.8eV. Acetylene-temperature programmed desorption (C_2H_2-TPD) measurements were performed on a FINESORB-3010 chemisorption analyzer. Briefly, the samples (50 mg) were first treated with Ar gas at 200 °C for 1.5 h. After cooling, it was continually flushed with a C_2H_2 flowing at a rate of 25 mL·min^{-1} and heated from room temperature to 500 °C at a heating rate of 10 °C·min^{-1}. The coke deposition of spent catalysts were determined by thermogravimetric analysis (TG) instruments (NETZSCH STA 449F3) over the temperature from atmosphere temperature to 800 °C at a heating rate of 15 °C·min^{-1} and an air flow rate of 30 mL·min^{-1}. HCl adsorption experiments were analyzed by titration method [22].

2.4. Catalyst tests

The hydrochlorination of acetylene tested in the fixed-bed micro-reactor (i.d.10 mm). The reaction temperature was regulated using a temperature controller (Yudian Al-808H). When the reactor temperature initially was maintained at 180 °C, the hydrogen chloride firstly fed into the reactor containing 4 mL catalysts to get rid of moistures and air in reaction

system for 30 min. The mole ratio of C_2H_2/HCl=1.0:1.1 was calibrated by mass flow controller with a given C_2H_2-GHSV of 30 h^{-1}. Then, the product mixture gas was getting through the medical soda lime to remove the unreacted hydrogen chloride. The final product gas was analyzed by an online gas chromatograph (GC900) using TCD as the detector for gas chatomatograph, which equipped with a packed column (GDX301).

3. Results and discussion

3.1. Physicochemical properties of NCDs

Figure 1a shows that the XRD patterns of NCDs displays a broad peak at 23.8°, suggesting that NCDs is mainly composed of amorphous carbon [33–35]. Figure 1b shows the FT-IR spectra of NCDs, with four characteristic peaks at 3195, 3055, 1651 and 1567 cm^{-1} inferring the bonding formation of -CO-NH- [26]. The composition of NCDs was studied by XPS. The full scan spectra of XPS confirm the existence of C, N and O in NCDs (Figure 1c). The high-resolution N_{1s} is depicted in Figure 1d, three peaks at 399.6 eV, 400.5 eV and 401.7 eV that commonly correspond to C-N-C, N-$(C)_3$ and N-H, respectively [27,36] (Figure 1e). In the XPS-C_{1s} spectra of NCDs, the deconvoluted three peaks at 284.5 eV, 286.0 eV, and 288.4 eV can be assigned to C=C, C-N, and N-C=N, respectively [26,36]. Moreover, two types oxygen species at 531.8 eV (C=O) and 533.3 eV (C-OH/C-O-C) are observed in the sample (Figure 1f) [36,37]. Based on both FTIR and XPS results, the successful synthesis of NCDs was confirmed.

3.2. Catalytic performance

The effect of NCDs on the performances of $(C_6H_5)Cl_3Sn$/AC catalysts was evaluated at a temperature of 180 °C with C_2H_2-GHSV of 30 h^{-1}, and the results is displayed in Figure 2a. The acetylene conversion of 5%$(C_6H_5)Cl_3Sn$/NCDs@AC, 10%$(C_6H_5)Cl_3Sn$/NCDs@AC, 15%$(C_6H_5)Cl_3Sn$/NCDs@AC, and 20%$(C_6H_5)Cl_3Sn$/

NCDs@AC are 78.2%, 88.5%, 92.5%, and 87.3%, respectively, and 15%$(C_6H_5)Cl_3Sn$/NCDs@AC with highest acetylene conversion (92.5%) was selected for the following studies. The acetylene conversion of 15%$(C_6H_5)Cl_3Sn$/NCDs@AC and 15%$(C_6H_5)Cl_3Sn$/AC (90.2%) are similar, which prove that NCDs exhibits a little effect on the catalytic activity of $(C_6H_5)Cl_3Sn$/AC. Comparing with 15%$(C_6H_5)Cl_3Sn$/AC (90.2%), only 8.9% C_2H_2 has been transformed to vinyl chloride over AC and NCDs@AC features 17.9% acetylene conversion, suggesting that $(C_6H_5)Cl_3Sn$ can catalyze the acetylene hydrochlorination to generate vinyl chloride and NCDs doped-AC can enhance the catalytic performance of AC. At the same time, the VCM selectivity of five catalysts decrease in the following order: 15%$(C_6H_5)Cl_3Sn$/NCDs@AC (99.2%)> 15%$(C_6H_5)Cl_3Sn$/AC(98.5%)> NCDs@AC (78.8%)> AC (76.5%) (Figure 2b). Experiments show that the higher VCM selectivity of catalysts is mainly attributed to the $(C_6H_5)Cl_3Sn$.

As shown in Figure 2c, 15%$(C_6H_5)Cl_3Sn$/NCDs@AC features stable catalytic performance at first 12 h of the reaction. After 40 h since the reaction started, the acetylene conversion of 15%$(C_6H_5)Cl_3Sn$/NCDs@AC gradually decreases from 92.5% to 59.2%. However, 15%$(C_6H_5)Cl_3Sn$/AC reaches the acetylene conversion of 90.2% and then reduced by 66.1% 40 h after reaction. Furthermore, it is concluded that NCDs additives can prolong the lifetime of $(C_6H_5)Cl_3Sn$/AC catalysts for acetylene hydrochlorination. Figure 2d shows that the deactivation rate of 15%$(C_6H_5)Cl_3Sn$/AC (1.65 $\%\cdot h^{-1}$) is higher than that of 15%$(C_6H_5)Cl_3Sn$/NCDs@AC (0.82 $\%\cdot h^{-1}$), indirectly proving the above-mentioned conclusion.

3.3. Physical properties of catalysts

The specific surface area, pore volume, and pore size distribution of catalysts were analyzed by the nitrogen adsorption/desorption experiments. According to IUPAC classification (Figure 3a), all catalysts display the type-I langmuir isotherms and type H_4 loop, which suggests the coexistence of micro- and mesorpores in samples. This result is in compliance with the pore size distribution curves (Figure 3b). As listed in Table 1, the specific surface area of NCDs@AC, 15%$(C_6H_5)Cl_3Sn$/AC and 15%$(C_6H_5)Cl_3Sn$/NCDs@AC is 798 $cm^3\cdot g^{-1}$, 712 $cm^3\cdot g^{-1}$ and 631 $cm^3\cdot g^{-1}$, respectively, which are all lower than that of AC (983 $cm^3\cdot g^{-1}$), indicating that additives successfully loaded into carbon support. As can be seen in Figure 3c, the two obvious diffraction peaks at 26.4 and 44.4 ° correspond to the (002) and (101) crystal planes of AC (PDF#41-1487), respectively [38]. However, there are no other discernible peaks in 15%$(C_6H_5)Cl_3Sn$/NCDs@AC, inferring that $(C_6H_5)Cl_3Sn$ homogeneously dispersed on the NCDs@AC surface [39]. We analyzed the 15%$(C_6H_5)Cl_3Sn$/NCDs@AC and 15%$(C_6H_5)Cl_3Sn$/AC through TEM images (Figure 3d and Figure 3e). As depicted in Figure 3d, 15%$(C_6H_5)Cl_3Sn$/AC has some black particles, which represent that $(C_6H_5)Cl_3Sn$ dispersed on the carbon surface. In stark contrast, this phenomenon does not exist in 15%$(C_6H_5)Cl_3Sn$/NCDs@AC surface. This result suggests that NCDs@AC carrier can promote the better dispersion of $(C_6H_5)Cl_3Sn$.

3.4. Chemical properties of catalysts

The surface element composition of catalysts and the chemical effect of NCDs on $(C_6H_5)Cl_3Sn$ were investigated by XPS techniques. To be specific, Figure 4a and Table 2 prove that the element of Sn, N, C, Cl and O exist in four $(C_6H_5)Cl_3Sn$-based catalysts.

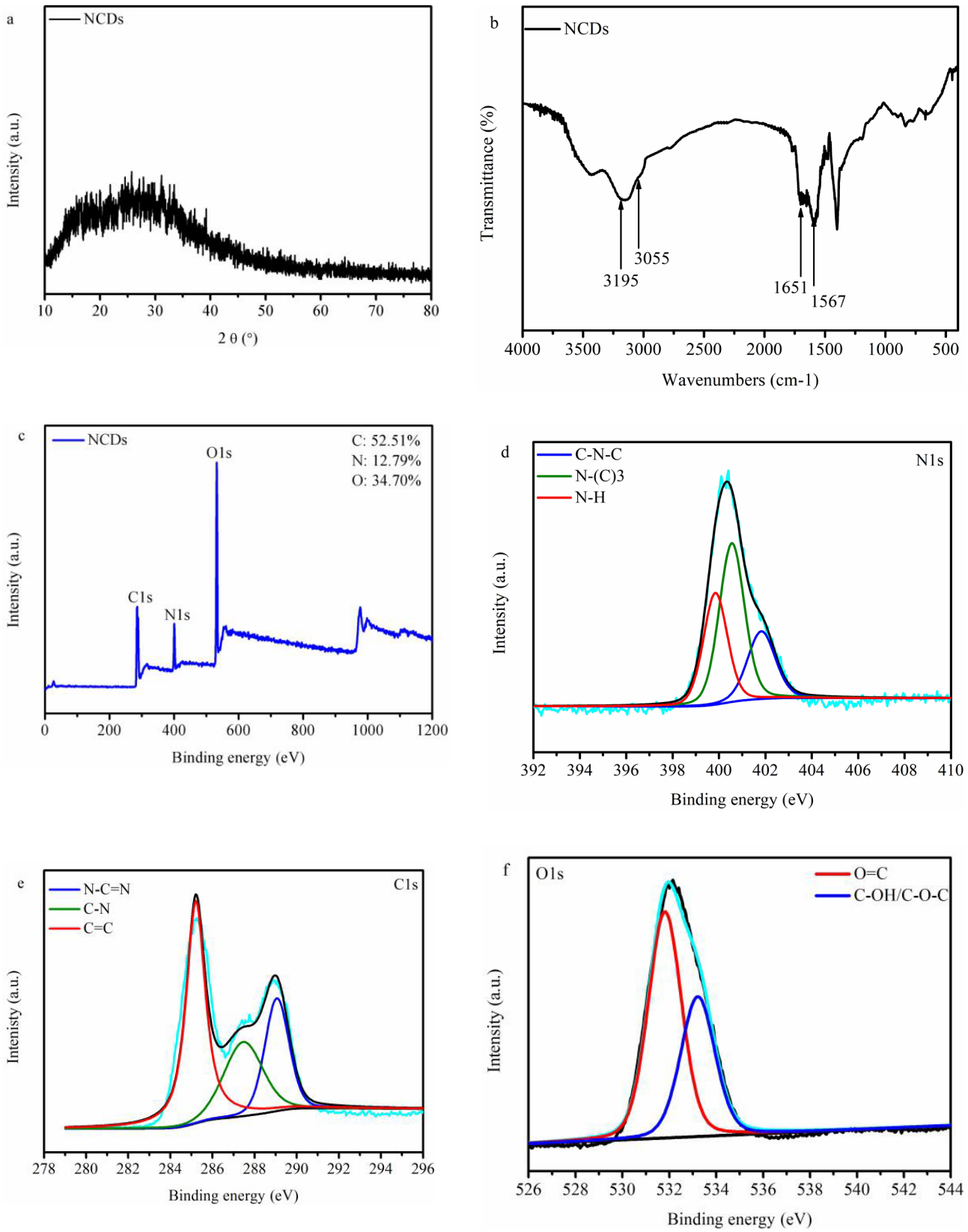

Figure 1. (a) XRD patterns of NCDs, (b) FTIR spectra of NCDs, (c) XPS patterns of NCDs, (d) High resolution XPS-C_{1s} spectra of NCDs, (e) High resolution XPS-N_{1s} spectra of NCDs, (f) High resolution XPS-O_{1s} spectra of NCDs.

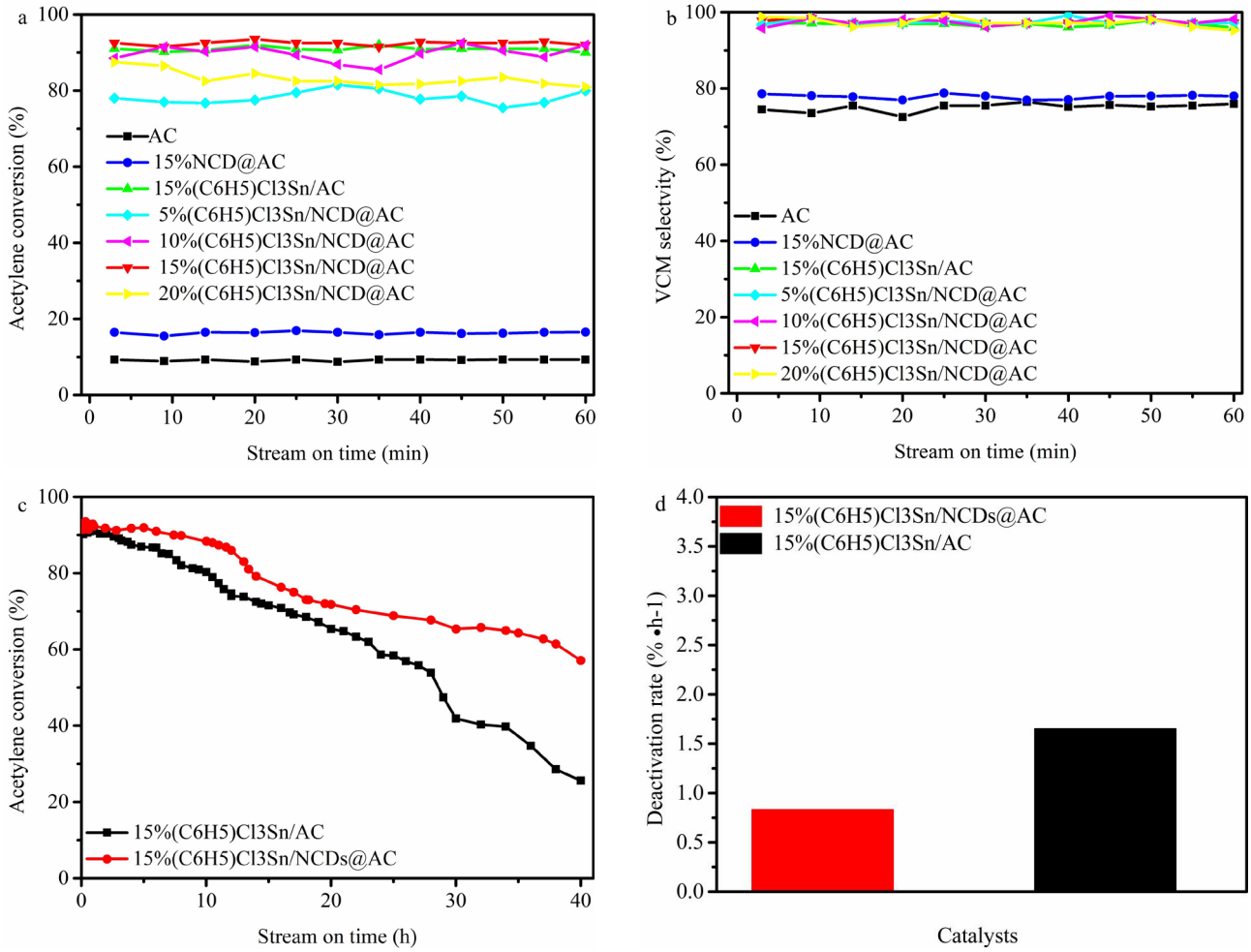

Figure 2. (a) Acetylene conversion and (b) VCM selectivity of different catalysts, (c) Stability of 15%$(C_6H_5)Cl_3Sn$/NCDs@AC and 15%$(C_6H_5)Cl_3Sn$/AC, (d) Deactivation rate of 15%$(C_6H_5)Cl_3Sn$/NCDs@AC and 15%$(C_6H_5)Cl_3Sn$/AC (Reaction condition: T=180 °C, C_2H_2-GHSV=30 h^{-1}, V_{HCl}/V_{C2H2}=1.1/1.0).

3.4.1. $Sn3_{d5/2}$

As shown in Figure 4b, the high resolution $Sn3_{d5/2}$ spectrum of 15%$(C_6H_5)Cl_3Sn$/AC reaches two peaks at 485.5 eV and 486.9 eV, which are related to the presence of Sn-C and Sn-O, respectively [40–43]. However, the high resolution $Sn3_{d5/2}$ spectrum in the case of 15%$(C_6H_5)Cl_3Sn$/NCDs@AC (Figure 4c) can be deconvoluted into three individual peaks corresponding to Sn-O (486.9 eV), Sn-C (485.5 eV) and Sn-N_x (486.0~486.8 eV) [42-45], confirming that the presence of Sn-N_x in catalysts is due to the interaction between $(C_6H_5)Cl_3Sn$ and NCDs .

Because a number of oxygen-containing functional groups on the AC and NCDs surface are able to react with NH_3 under 200 °C [46], fresh-15%$(C_6H_5)Cl_3Sn$/NCDs@AC (10.75 wt.%) surface has the lower oxygen element content than that of fresh-15%$(C_6H_5)Cl_3Sn$/AC (12.03 wt.%) (Table 2). However, in the catalytic acetylene hydrochlorination reaction, the reason of Sn-O in $(C_6H_5)Cl_3Sn$-based catalysts reacting with HCl may be to generate $SnCl_4$, which easily sublimes at 180 °C, resulting in the loss of Sn species (Table 3). As listed in Table 2, the Sn content in $(C_6H_5)Cl_3Sn$/AC decreased from 5.65 to 1.17 wt.% after 40 h of reaction. Interestingly, the only Sn amount of 2.92 wt.% was leached from 15%$(C_6H_5)Cl_3Sn$/NCDs@AC. Additionally, the Sn-N_x content in the case of 15%$(C_6H_5)Cl_3Sn$/NCDs@AC is reduced by 1.09 wt.% after 40 h (Table 4). The above analysis indicated that Sn-N_x stabilizes the loss of Sn species during the reaction (Figure 2c).

3.4.2. N_{1s}

It can be seen in Figure 4d that there are four fitted peaks (C-N-C (399.6 eV), N-$(C)_3$ (400.5 eV), N-H (401.7 eV) and N_x-Sn (397.7 eV)), in the N1s spectra of 15%$(C_6H_5)Cl_3Sn$/NCDs@AC [26,38,45], which represents that NCDs successfully dispersed on AC surface and also prove the existence of Sn-N_x.

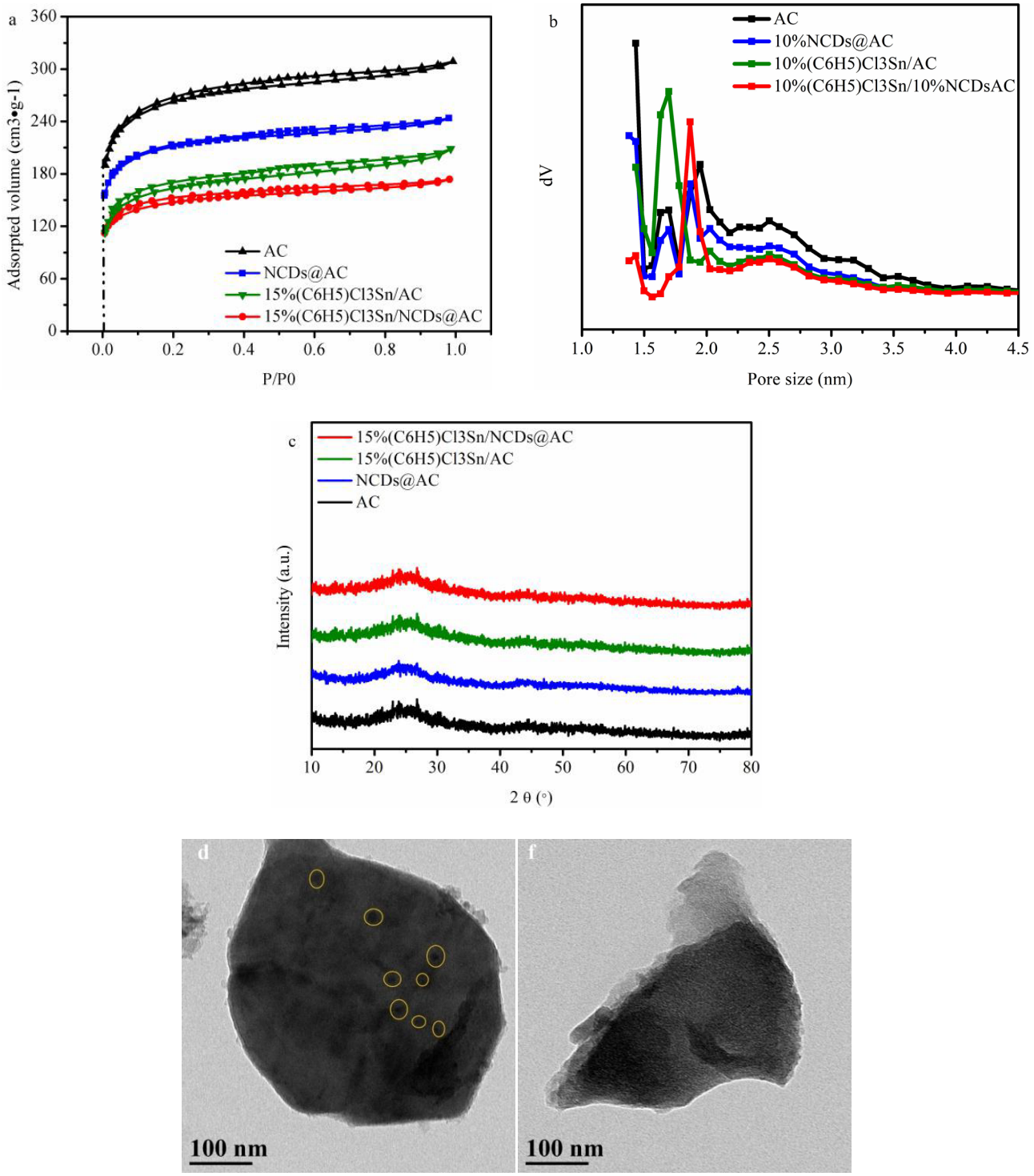

Figure 3. (a) Nitrogen adsorption/desorption isotherm of different catalysts; (b) Pore size distribution of different catalysts; (c) XRD pattern of different catalysts; TEM images of (d) 15%$(C_6H_5)Cl_3Sn$/AC; (e) 15%$(C_6H_5)Cl_3Sn$/NCDs@AC

The effect of NCDs on the reactants adsorption of $(C_6H_5)Cl_3Sn$-based catalysts was investigated by C_2H_2-TPD and hydrogen chloride adsorption/desorption experiments, respectively. The acetylene adsorption amounts of four catalysts are as follows: 15%$(C_6H_5)Cl_3Sn$/NCDs@AC> 15%$(C_6H_5)Cl_3Sn$/AC> NCDs@AC> AC (Figure 5a). Particularly, 15%$(C_6H_5)Cl_3Sn$/AC shows the stronger acetylene adsorption ability than that of AC. This implies that $(C_6H_5)Cl_3Sn$ displays a key role

Table 1. Texture parameters of catalysts and AC.

Samples	BET_{total}	BET_{meso}	BET_{micro}	V_{total}	D
	($cm^2 \cdot g^{-1}$)	($cm^2 \cdot g^{-1}$)	($cm^2 \cdot g^{-1}$)	($cm^3 \cdot g^{-1}$)	(nm)
AC	983	129	854	0.48	1.90
NCDs@AC	798	89	709	0.41	1.92
15%(C_6H_5)Cl_3Sn/AC	712	106	606	0.38	2.00
15%(C_6H_5)Cl_3Sn/NCDs@AC	631	103	528	0.30	2.20

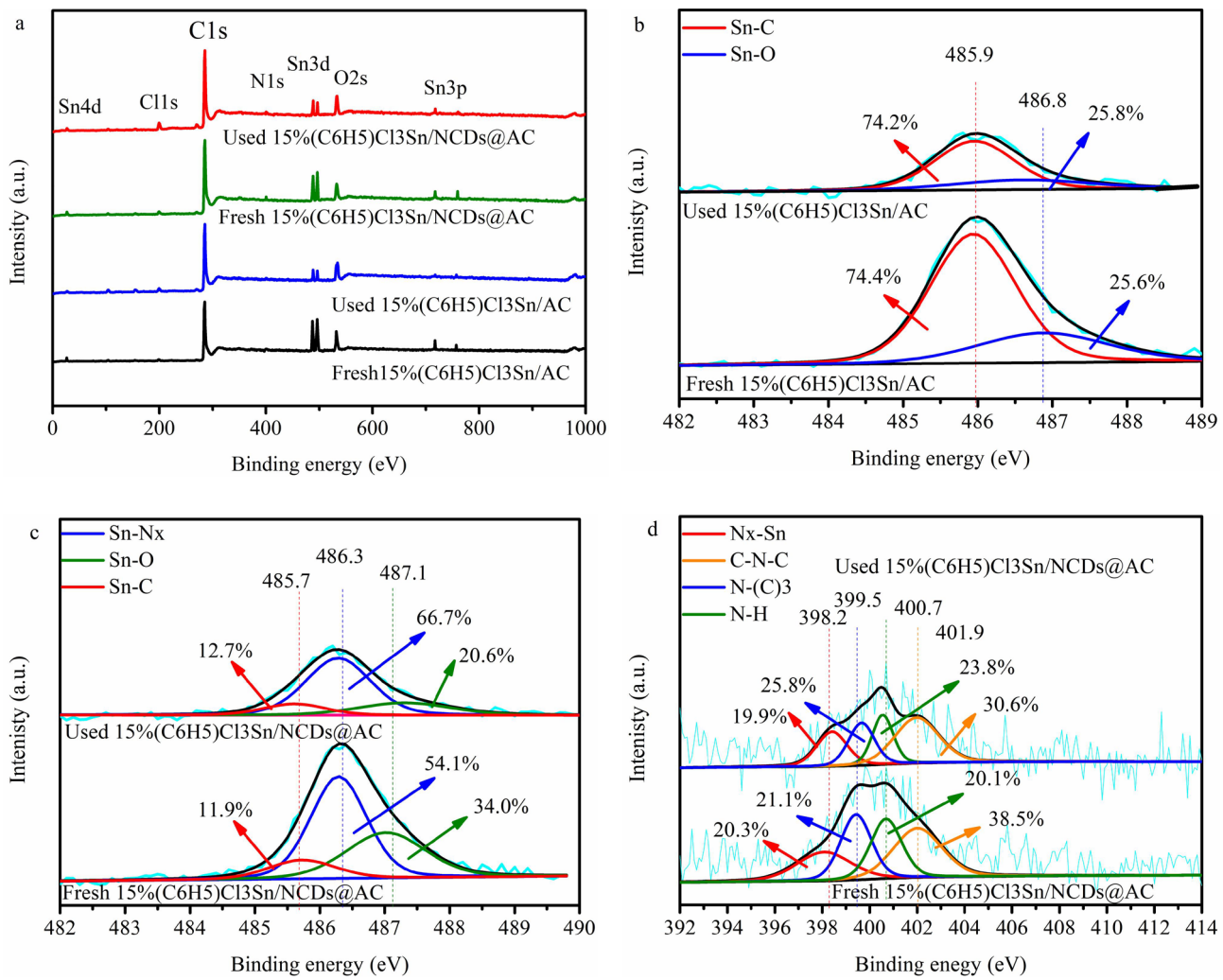

Figure 4. (a) XPS pattern of different catalysts, (b) High resolution XPS spectra of $Sn3d_{5/2}$ in fresh- and used 15%(C_6H_5)Cl_3Sn/AC, (c) High resolution XPS spectra of $Sn3d_{5/2}$ in fresh- and used 15%(C_6H_5)Cl_3Sn/NCDs@AC, (d) High resolution XPS spectra of N1s in fresh- and used 15%(C_6H_5)Cl_3Sn/NCDs@AC.

in acetylene adsorption. As illustrated in Figure 5b, 15%(C_6H_5)Cl_3Sn/NCDs@AC, 15%(C_6H_5)Cl_3Sn/AC, NCDs@AC, and AC feature the hydrogen chloride adsorption amount of 0.23 $mmol \cdot g^{-1}$, 0.21 $mmol \cdot g^{-1}$, 0.19 $mmol \cdot g^{-1}$ and 0.18 $mmol \cdot g^{-1}$, respectively (Table 5,6,7,8). Compared to bare AC, the higher content of Pyridine N in NCDs@AC plays a key role on the hydrogen chloride adsorption [47,48]. Furthermore, the hydrogen chloride adsorption of 15%(C_6H_5)Cl_3Sn/NCDs@

Table 2. The relative contents of different elements in catalysts.

Sample	Elements (wt%)				
	Sn	N	C	O	Cl
Fresh 15%$(C_6H_5)Cl_3Sn$/AC	5.65	0.44	77.84	12.03	4.04
Used 15%$(C_6H_5)Cl_3Sn$/AC	1.17	0.58	79.72	11.48	7.05
Fresh15%$(C_6H_5)Cl_3Sn$/NCDs@AC	5.69	2.36	78.01	10.75	3.19
Used15%$(C_6H_5)Cl_3Sn$/NCDs@AC	2.92	2.04	79.95	11.02	4.07

Table 3. The relative contents of Sn-O in catalysts.

Sample	Total Sn-O content (wt%)		Loss (wt %)
	Fresh	Used	△Sn-O
15%$(C_6H_5)Cl_3Sn$/AC	1.45	0.30	1.15
15%$(C_6H_5)Cl_3Sn$/NCDs@AC	1.93	0.60	1.33

Table 4. The relative contents of Sn-N_x in catalysts.

Sample	Total Sn-N_x content(wt%)		Loss (wt %)
	Fresh	Used	△Sn-N_x
15%$(C_6H_5)Cl_3Sn$/AC	--	--	--
15%$(C_6H_5)Cl_3Sn$/NCDs@AC	3.07	1.98	1.09

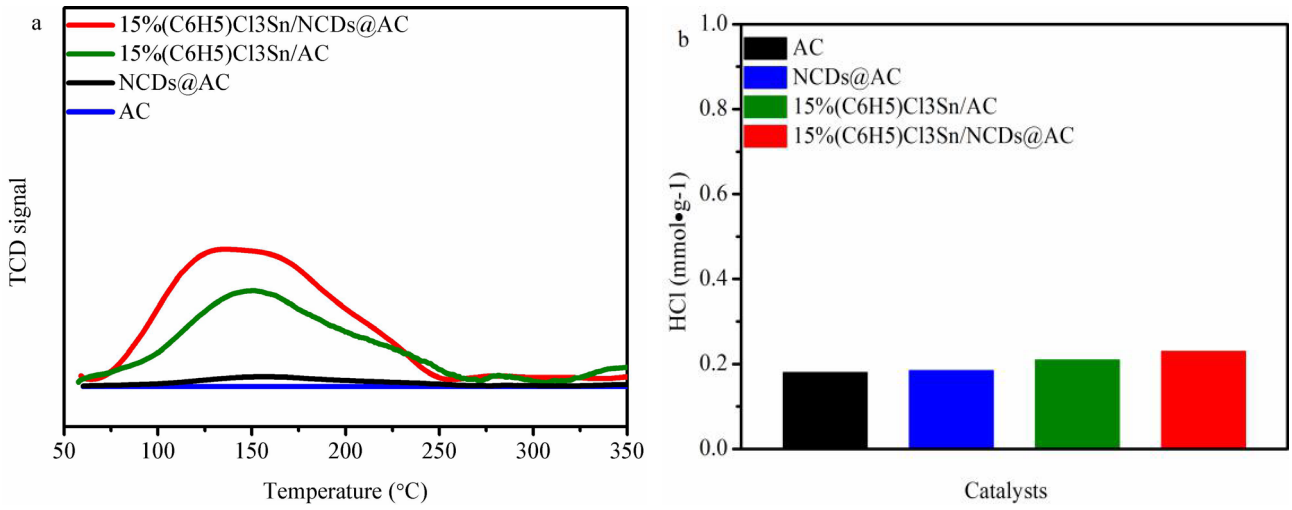

Figure 5. (a) C_2H_2-TPD of catalysts, (b) HCl adsorption of catalysts.

AC is higher than that of 15%$(C_6H_5)Cl_3Sn$/AC. It is indicated that NCDs additives can promote the hydrogen chloride adsorption of $(C_6H_5)Cl_3Sn$/NCDs@AC, as result of the coexistence of Sn-N_x and Pyridine N (Figure 5b and Figure 4).

3.5. Deactivation reason

The specific surface area of 15%$(C_6H_5)Cl_3Sn$/AC and 15%$(C_6H_5)Cl_3Sn$/10%NCDs@AC is reduced by 447 $cm^2\ g^{-1}$ and 328 $cm^2\ g^{-1}$ after 40 h of reaction, respectively (Table 9) indicates indirectly that coke deposition is one of deactivation reason of

Table 5. The different parameter of 15%$(C_6H_5)Cl_3Sn$/NCDs@AC.

Numbers	Na_2CO_3 (mL)	Adsorption volume (mL)	Catalysts (g)	HCl adsorption capacity (mmol g^{-1})
1	10530	250	3.51	0.24
2	10033	250	3.49	0.23
3	9652	250	3..51	0.22
4	10063	250	3.50	0.23

Table 6. The different parameter of 15%$(C_6H_5)Cl_3Sn$/AC.

Numbers	Na_2CO_3 (mL)	Adsorption volume (mL)	Catalysts (g)	HCl adsorption capacity (mmol g^{-1})
1	8625	250	3.45	0.20
2	9004	250	3.43	0.21
3	9082	250	3.46	0.21
4	8600	250	3.44	0.20

Table 7. The different parameter of NCDs@AC.

Numbers	Na_2CO_3 (mL)	Adsorption volume (mL)	Catalysts (g)	HCl adsorption capacity (mmol g^{-1})
1	8075	250	3.40	0.19
2	8099	250	3.41	0.19
3	8550	250	3.42	0.20
4	7695	250	3.42	0.18

Table 8. The different parameter of AC.

Numbers	Na_2CO_3 (mL)	Adsorption volume (mL)	Catalysts (g)	HCl adsorption capacity (mmol g^{-1})
1	7203	250	3.39	0.17
2	7225	250	3.40	0.17
3	7456	250	3.41	0.19
4	7650	250	3.40	0.18

$(C_6H_5)Cl_3Sn$/AC in the hydrochlorination of acetylene [49]. Additionally, all the number of tin species in different catalysts decreased promptly in Table 1, which shows that another deactivation occurs from the loss of tin species.

3.6. Catalysis mechanism

The C_2H_2-TPD, FT-IR, HCl adsorption/desorption experiments and Rideal–Eley mechanism [50,51] were used to investigate the reaction mechanism of $(C_6H_5)Cl_3Sn$/AC in acetylene hydrochlorination. In addition, $(C_6H_5)Cl_3Sn$/AC was separately pretreated with HCl, C_2H_2 and N_2 at 180 °C for 1 h. Later on, $(C_6H_5)Cl_3Sn$/AC-HCl, $(C_6H_5)Cl_3Sn$/AC-C_2H_2, $(C_6H_5)Cl_3Sn$/AC-N_2 were characterized by FT-IR techniques. Both $SnCl_4$ and HCl as electron-acceptor do not react with each other [52], and $(C_6H_5)Cl_3Sn$ is more inclined to adsorb acetylene rather than HCl (Figure 5a, b). The above-mentioned two points infer that $(C_6H_5)Cl_3Sn$ prefers to interact with C_2H_2 in the catalytic acetylene hydrochlorination process. However, only one characteristic adsorption bands at ~1610 cm^{-1} is observed in $(C_6H_5)Cl_3Sn$/AC-C_2H_2, suggesting

that the existence of -C=C- consequently infers the interaction between gaseous C_2H_2 and $(C_6H_5)Cl_3Sn$ (Figure 6) [53,54]. This result suggests that the $(C_6H_5)Cl_3Sn$ does interact with C_2H_2, and $(C_6H_5)Cl_3Sn/AC\text{-}C_2H_2$ is transition state of $(C_6H_5)Cl_3Sn$ in catalysis acetylene hydrochlorination reaction and then adsorbs HCl to generate vinyl chloride. Based on the analysis of previous studies, the reactant adsorption ability of catalysts displays a vital in acetylene hydrochlorination, but strong C_2H_2 adsorption may result in deactivation of the catalysts [55–57]. Accordingly, it is proposed that coke deposition is main deactivation reason for $(C_6H_5)Cl_3Sn$-based catalysts in the hydrochlorination of acetylene. It can be seen from Figure 4b, the binding energy of the Sn-C ($Sn3_{d5/2}$) in $(C_6H_5)Cl_3Sn$/NCDs@AC is centered at 485.7 eV, but $(C_6H_5)Cl_3Sn$/AC is located at 485.9 eV. This negative shift is due to Sn-N_x (Figure 4c). Significantly, this results promote the hydrogen chloride adsorption of $(C_6H_5)Cl_3Sn$/NCDs@AC and, therefore, improve the catalytic performance of $(C_6H_5)Cl_3Sn$-based catalysts in the acetylene hydrochlorination reaction.

4. Conclusion

In conclusion, $(C_6H_5)Cl_3Sn$/AC can catalyze the acetylene hydrochlorination process. The intermolecular force between $(C_6H_5)Cl_3Sn$ and NCDs induces the formation of Sn-N_x, which can promote the $(C_6H_5)Cl_3Sn$ dispersion, reduce the $(C_6H_5)Cl_3Sn$ loss and lessen coke deposition, leading to the longer lifetime of $(C_6H_5)Cl_3Sn$/AC. According to the Rideal–Eley mechanism and experiments results, we proposed that the $(C_6H_5)Cl_3Sn/AC\text{-}C_2H_2$ indicates a transition state of $(C_6H_5)Cl_3Sn$ in catalysis of acetylene hydrochlorination reaction and then adsorbs HCl to generate vinyl chloride. Thus, it is showed that the main deactivation reason of $(C_6H_5)Cl_3Sn$/AC is coke deposition during the acetylene hydrochlorination. This work provides a novel application of $(C_6H_5)Cl_3Sn$ and NCDs for further studies on the organotin-based catalysts for acetylene hydrochlorination.

Table 9. Specific surface area of fresh- and used catalysts.

Sample	$S_{BET}(cm^2g^{-1})$		$S_{\triangle BET}(cm^2g^{-1})$
	fresh	used	
15%$(C_6H_5)Cl_3Sn$/AC	712	265	447
15%$(C_6H_5)Cl_3Sn$/NCDS@AC	631	303	328

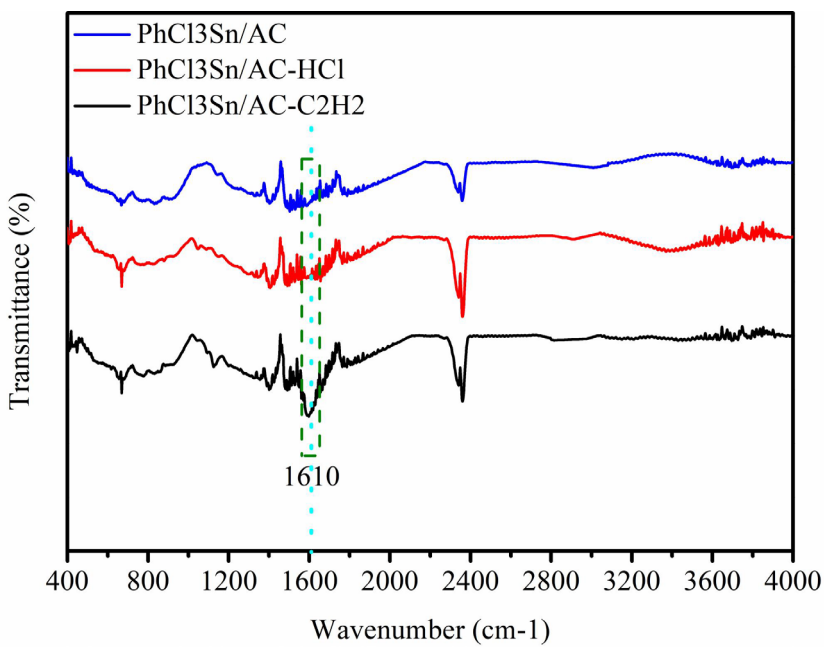

Figure 6. FTIR spectra of different $(C_6H_5)Cl_3Sn$/AC

Acknowledgments
This work is supported by PhD research startup foundation of Pingding Shan University (PXY-BSQD-202110).
This study was supported by Natural Science Foundation of Guizhou ([2019]2872 and [2020]1Y037), Guizhou Education Department Youth Science and Technology Talents Growth Project (QianJiaoHe KY [2021]253), Science and Technology Supporting Foundation of Liupanshui (52020-2018-01-04, H2020-003).

References

1. Ingham RK, Rosenberg SD, Gilman H. Organotin Compounds. Chemical Reviews 1960; 60: 459-539. doi: 10.1021/cr60207a002
2. Gielen M. Tin-based antitumour drugs. Coordination Chemistry Reviews, 1996; 151: 41-51. doi: 10.1155/mbd.1994.213
3. Yang P, Guo M. Interactions of organometallic anticancer agents with nucleotides and DNA. Coordination Chemistry Reviews 1999; 185: 189-211. doi: 10.1016/S0010-8545(98)00268-9
4. Alama A, Tasso B, Novelli F, Sparatore F. Organometallic compounds in oncology: implications of novel organotins as antitumor agents. Drug Discovery Today 2009; 14: 500-508. doi: 10.1016/j.drudis.2009.02.002
5. Champ MA. A review of organotin regulatory strategies, pending actions, related costs and benefits. Science of the Total Environment 2000; 258: 21-71. doi: 10.1016/S0048-9697(00)00506-4
6. Ayrey G, Hsu SY, Poller RC. The use of organotin compounds in the thermal stabilization of poly(vinyl chloride). VI. an assessment of the relative importance of HCl-scavenging, exchange, and addition reactions. Journal of Polymer Science Part A-Polymer Chemistry 1984; 22: 2871-2886. doi: 10.1002/pol.1984.170221112
7. Song J, Zhang B, Wu T, Yang G, Han B. Organotin-oxomolybdate coordination polymer as catalyst for synthesis of unsymmetrical organic carbonates. Green Chemistry 2011; 13: 922-927. doi: 10.1039/C0GC00765J
8. da Silva MA, dos Santos ASS, dos Santos TV, Meneghetti MR, Meneghetti SMP. Organotin(iv) compounds with high catalytic activities and selectivities in the glycerolysis of triacylglycerides. Catalysis Science & Technology 2017; 7: 5750-5757. doi: 10.1039/C7CY01559C
9. Iwasaki F, Maki T, Onomura O, Nakashima W, Matsumura Y. ChemInform Abstract: chemo-and stereoselective monobenzoylation of 1,2-diols catalyzed by organotin compounds. Journal of Organic Chemistry 2000; 65: 996-1002. doi: 10.1002/chin.200021070
10. Khattak ZAK, Younus HA, Ahmad N, Yu B, Ullah H et al. Mono-and dinuclear organotin (IV) complexes for solvent free cycloaddition of CO_2 to epoxides at ambient pressure. Journal of CO_2 Utilization 2018; 28: 313-318. doi: 10.1016/j.jcou.2018.10.014
11. Wu YB, Li BW, Li FX, Xue JW, Lv ZP. Synthesis and characteristics of organotin-based catalysts for acetylene hydrochlorination. Canadian Journal of Chemistry 2018; 96: 447-452. doi: 10.1139/cjc-2017-0612
12. Wu YB, Li FX, Xue JW, Lv ZP. Effect of various g-C_3N_4 precursors on the catalytic performance of alkylorganotin-based catalysts in acetylene hydrochlorination, Turkish Journal of Chemistry 2020; 44: 393-408. doi: 10.3906/kim-1909-64
13. Schobert H. Production of acetylene and acetylene-based chemicals from coal. Chemical Reviews 2013; 114: 1743-1760. doi: 10.1021/cr400276u
14. Gustin MS, Amos HM, Huang J, Matthieu BM, Keith H. Measuring and modeling mercury in the atmosphere: a critical review. Atmospheric Chemistry and Physics 2015; 15: 5697-5713. doi: 10.5194/acp-15-5697-2015
15. Harris HH, Pickering IJ, George GN. The chemical form of mercury in fish. Science 2013; 301: 1203-1203. doi: 10.1126/science.1085941
16. Deng GC, Wu BX, Li TS, Liu GD, Wang LF et al. Preparation of solid phase non mercury catalyst for synthesis of vinyl chloride by acetylene method. Polyvinyl chloride 1994; 6: 5-9. http://www.cnki.com.cn/Article/CJFDTotal-JLYA199406001.htm
17. Gao SL, Sun X, Lv ZL, Qin YC, Zhang XT et al. The application of Sn-Bi-Co@AC catalysts for acetylene hydrochlorination. Journal of Petrochemical Universities, 2016; 29: 1-5. doi: 10.3969/j.issn.1006-396X.2016.02.001
18. Zhag L, Jiang H, Wang H, Dong SW, Ding LW et al. Preparation and application of non-mercury catalysts for acetylene hydrochlorination. Journal of Petrochemical Universities 2013; 26: 6-11. doi: 10.3969/j.issn.1006-396X.2013.06.002
19. Xiong Q, Wu GW, Ling S, Xiong Z, Hu ZP et al. Preparation and optimization of mercury-free catalyst for synthesis of vinyl chloride from acetylene. Modern Chemical Industry 2007; 37: 66-69. doi:10.16606/j.cnki.issn0253-4320.2017.11.015
20. Guo YY, Liu Y, Hu RS, Gao GJ, Sun HJ. Preparation and optimization of $SnCl_2$-$ZnCl_2$/C mercury-free catalyst for acetylene hydrochlorination. Chinese Journal of Applied Chemistry 2014; 31: 624-626. doi: 10.3724/SP.J.1095.2014.30337
21. Wu YB, Li FX, Lv ZP, Xue JW. Carbon-supported binary Li-Sn catalyst for acetylene hydrochlorination. Journal of Saudi Chemical Society 2019; 19: 002. doi: 10.1016/j.jscs.2019.08.002

22. Wu YB, Li FX, Xue JW, Lv ZP. Sn-imidazolates supported on boron and nitrogen-doped activated carbon as novel catalysts for acetylene hydrochlorination. Chemical Engineering Communications 2019; 207: 1203-1215. doi: 10.1080/00986445.2019.1641700

23. Li X, Wang Y, Kang L, Zhu M, Dai B. A novel, non-metallic graphitic carbon nitride catalyst for acetylene hydrochlorination. Journal of Catalysts 2014; 311: 288-294. doi: 10.1016/j.jcat.2013.12.006

24. Lin R, Kaiser SK, Hauert R, Ramírez JP. Descriptors for high-performance nitrogen-doped carbon catalysts in acetylene hydrochlorination. ACS Catalysis 2018; 8: 1114-1121. doi: 10.1021/acscatal.7b03031

25. Li X, Zhu M, Dai B. $AuCl_3$ on polypyrrole-modified carbon nanotubes as acetylene hydrochlorination catalysts. Applied Catalysis, B: Environmental 2013; 142: 234-240. doi: 10.1016/j.apcatb.2013.05.031

26. Zhang R, Chen W. Nitrogen-doped carbon quantum dots: Facile synthesis and application as a"turn-off"fluorescent probe for detection of Hg^{2+} ions. Biosensors & Bioelectronics 2014; 55: 83-90. doi: 10.1016/j.bios.2013.11.074

27. Yang Z, Xu M, Liu Y, He F, Gao F et al. Nitrogen-doped, carbon-rich, highly photoluminescent carbon dots from ammonium citrate. Nanoscale 2014; 6: 1890-1895. doi: 10.1039/C3NR05380F

28. Dong Y, Pang H, Yang HB, Guo CX, Shao JW et al. Carbon-based dots Co-doped with nitrogen and sulfur for high quantum yield and excitation-independent emission. Angewandte Chemie International Edition 2013; 52: 7800-7804. doi:10.1002/anie.201301114

29. Choi Y, Kang B, Lee J, Kim S, Kim GT et al. Integrative approach toward uncovering the origin of photoluminescence in dual heteroatom-doped carbon nanodots. Chemistry of Materials 2016; 28: 6840-6847. doi: 10.1021/acs.chemmater.6b01710

30. Lin C, Zhuang Y, Li W, Zhou TL et al. Blue, green, and red full-color ultralong afterglow in nitrogen-doped carbon dots. Nanoscale 2019; 11: 6584-6590. doi: 10.1039/C8NR09672D

31. Yue YX, Wang BL, Wang SS, Jin CX, Lu JY et al. Boron-doped carbon nanodots dispersed on graphitic carbon as high-performance catalysts for acetylene hydrochlorination. Chemical Communication 2020; 56: 5174-5177. doi: 10.1039/C9CC09701E

32. Tian Z, Tian P, Zhou X, Zhou G, Mei S et al. Ultraviolet-pumped white light emissive carbon dot based phosphors for light-emitting devices and visible light communication. Nanoscale 2019; 11: 3489-3494. doi: 10.1039/C9NR00224C

33. Qu S, Wang X, Lu Q, Liu X, Wang L. A biocompatible fluorescent ink based on water-soluble luminescent carbon nanodots. Angewandte Chemie International Edition 2012; 51: 12215-12218. doi: 10.1002/anie.201206791

34. Wang F, Chen P, Feng Y, Xie Z, Liu Y et al. Facile synthesis of N-doped carbon dots/g-C_3N_4 photocatalyst with enhanced visible-light photocatalytic activity for the degradation of indomethacin. Applied Catalysis B: Environmental 2017; 207: 103-113. doi: 10.1016/j.apcatb.2017.02.024

35. Zhu S, Meng Q, Wang L, Zhang J, Song Y et al. Highly photoluminescent carbon dots for multicolor patterning, sensors, and bioimaging. Angewandte Chemie International Edition 2013; 52: 3953-3957. doi: 10.1002/anie.201300519

36. Fang S, Xia Y, Lv K, Li Q, Sun J et al. Effect of carbon-dots modification on the structure and photocatalytic activity of g-C_3N_4. Applied Catalysis B: Environmental 2015; 185: 225-232. doi: 10.1016/j.apcatb.2015.12.025

37. Gao Z, Lin Z, Chen X, Zhang H, Huang Z, A fluorescent probe based on N-doped carbon dots for highly sensitive detection of Hg^{2+} in aqueous solutions. Analytical Methods 2016; 8: 2297-2304. doi :10.1039/C5AY03088A

38. Qian H, Han H, Zhang F, Guo B, Yue Y et al. Non-catalytic CVD preparation of carbon spheres with a specific size. Carbon 2004; 42: 761-766. doi: 10.1016/j.carbon.2004.01.004

39. Zhang H, Li W, Jin Y, Sheng W, Hu M et al. Ru-Co(III)-Cu(II)/SAC catalyst for acetylene hydrochlorination. Applied Catalysis B: Environmental 2016; 189: 56-64. doi: 10.1016/j.apcatb.2016.02.030

40. Moulder JF, Stickle WF, Sobol PE, Bomben KE. Photochemical reduction of carbonate to formaldehyde on TiO_2 powder. Chemical Physics Letters 1995; 220: 7-10. doi: 10.1016/0009-2614(83)80259-0

41. Renard L, Babot O, Saadaoui H. Nanoscaled tin dioxide films processed from organotin-based hybrid materials: an organometallic route toward metal oxide gas sensors. Nanoscale 2012; 4: 6806-6813. doi: 10.1039/c2nr31883k

42. Larciprete R, Borsella E, De Padova P, Faglia G, Sberveglieri G. Organotin films deposited by laser-induced CVD as active layers in chemical gas sensors. Thin Solid Films 1998; 323: 291-295. doi: 10.1016/s0040-6090(97)01201-7

43. De Padova P, Fanfoni M, Larciprete R, Mangiantini M, Priori S et al. A synchrotron radiation photoemission study of the oxidation of tin. Surface Science 1994; 313: 379-391. doi: 10.1016/0039-6028(94)90058-2

44. Lewin E, Patscheider J. Structure and properties of sputter-deposited Al-Sn-N thin films. Journal of Alloys and Compounds 2016; 682: 42-51. doi: 10.1016/J.JALLCOM.2016.04.278

45. Inoue Y, Nomiya M, Takai O, Inoue Y, Nomiya M et al. Physical properties of reactive sputtered tin-nitride thin films. Vacuum 1998; 51: 673-676. doi: 10.1021/j100214a022

46. Vinke P, Eijk MVD, Verbree M, Voskamp AF, van Bekkum H. Modification of the surfaces of a gas-activated carbon and a chemically activated carbon with nitric acid, hypochlorite, and ammonia. Carbon 1994; 32: 675-686. doi: 10.1016/0008-6223(94)90089-2

47. Dai B, Chen K, Wang Y, Kang LH, Zhu MY. Boron and nitrogen doping in graphene for the catalysis of acetylene hydrochlorination. ACS Catslysis 2015; 5: 2541-2547. doi: 10.1021/acscatal.5b00199

48. Shen Z, Zhao H, Liu Y, Kan ZY, Xing P et al. Mercury-free nitrogen-doped activated carbon catalyst: an efficient catalyst for the catalytic coupling reaction of acetylene and ethylene dichloride to synthesize the vinyl chloride monomer. Reaction Chemistry & Engineering 2018; 3: 34-40. doi: 10.1039/C7RE00201G

49. Nkosi B, Adams MD, Coville NJ, Hutchings GJ. Hydrochlorination of acetylene using carbon-supported gold catalysts: a study of catalyst reactivation. Journal of Catalysis 1991; 128: 378-386. doi: 10.1016/0021-9517(91)90296-G

50. Bremer H, Lieske H. Kinetics of the hydrochlorination of acetylene on $HgCl_2$/active carbon catalysts. Applied Catalysis 1985; 18: 191. doi: 10.1016/S0166-9834(00)80308-5

51. Qi H, Li Q, Mo ZS, Zhang XT, Song LJ. MCl_2 (M=Hg, Cd, Zn, Mn) catalysed hydrochlorination of acetylene-a density functional theory study. Molecular Simulation 2017; 43: 28-33. doi: 10.1080/08927022.2016.1227076

52. Kowalewska E, Błaz˚ ejowski J, Thermochemical properties of H_2SnCl_6 complexes. Part I. Thermal behaviour of primary n-alkylammonium hexachlorostannates. Thermochimica Acta 1986; 101: 271-289. doi: 10.1016/0040-6031(86)80059-4

53. Andrews L, Johnson GL, Kelsall BJ. Fourier transform infrared matrix infrared spectra of the C_2H_2-HX and C_2H_X-HX hydrogen-bonded complex. The Journal of Physical Chemistry 1982; 86: 3374-3380. doi: 10.1021/j100214a022

54. Huber S, Knözinger H. Adsorption of CH-acids on magnesia: An FTIR-spectroscopic study. Journal of Molecular Catalysis A: Chemical 1999; 141: 117-127. doi: 10.1016/S1381-1169(98)00255-6

55. Hu J, Yang Q, Yang L, Zhang Z, Su B et al. Confining noble metal (Pd, Au, Pt) nanoparticles in surfactant ionic liquids: active non-mercury catalysts for hydrochlorination of acetylene, ACS Catalysis 2015; 5: 6724-6731. doi: 10.1021/acscatal.5b01690

56. Shang S, Zhao W, Wang Y, Li X, Zhang J et al. Highly efficient Ru@IL/AC to substitute mercuric catalyst for acetylene hydrochlorination. ACS Catalysis 2017; 7: 510-3520. doi: 10.1021/acscatal.7b00057

57. Ren Y, Wu B, Wang F, Li H, Lv G et al. Chlorocuprate(i) ionic liquid as an efficient and stable Cu-based catalyst for hydrochlorination of acetylene. Catalysis Science & Technology 2019; 9: 2868-2878. doi: 10.1039/C9CY00401G